https://doi.org/10.5194/hess-2021-264
Preprint. Discussion started: 25 May 2021

Hydrology and Earth System Sciences Discussions
Open Access

Diagnosing the impacts of permafrost on catchment hydrology: field measurements and model experiments in a mountainous catchment in western China

Hongkai Gao 1, 2*, Chuntan Han 3, Rensheng Chen 3, Zijing Feng 2, Kang Wang 1,2, Fabrizio Fenicia 4, Hubert Savenije 5

1 Key Laboratory of Geographic Information Science (Ministry of Education of China), East China Normal University, Shanghai, China

2 School of Geographical Sciences, East China Normal University, Shanghai, China

3 Qilian Alpine Ecology and Hydrology Research Station, Key Lab. of Ecohydrology of Inland River Basin, Northwest Institute of Eco-Environment and Resources, Chinese Academy of Sciences, Lanzhou 730000, China

4 Eawag, Swiss Federal Institute of Aquatic Science and Technology, Dubendorf, Switzerland

5 Delft University of Technology, Delft, the Netherlands

*Corresponding to: Hongkai Gao (hkgao@geo.ecnu.edu.cn)

Abstract:

Increased attention directed at permafrost hydrology has been prompted by climate change. In spite of an increasing number of field measurements and modeling studies, the impacts of permafrost on hydrological processes at the catchment scale are still unclear. Permafrost hydrology models at the catchment scale were mostly developed based on a "bottom-up" approach, hence by aggregating prior knowledge at the spot/field scales. In this study, we followed a "top-down" approach to learn from field measurement data to understand permafrost hydrology at the catchment scale. In particular, we used a stepwise model development approach to examine the impact of permafrost on streamflow response in the Hulu catchment in western China. We started from a simple lumped model (FLEX-L), and step-wisely included additional complexity by accounting for topography (i.e. FLEX-D) and landscape heterogeneity (i.e. FLEX-Topo). The final FLEX-Topo model, was then analyzed using a dynamic identifiability analysis (DYNIA) to investigate parameters' temporal variation. By enabling temporal dynamics on several parameters, we diagnosed the physical relationships between parameter variation and permafrost impacts. We found that in the Hulu catchment: 1) the improvement associated to the model modifications

https://doi.org/10.5194/hess-2021-264
Preprint. Discussion started: 25 May 2021

suggest that topography and landscape heterogeneity are dominant controls on catchment response; 2) baseflow recession in permafrost regions is the result of a linear reservoir, and slower than non-permafrost regions; 3) parameters variation infers seasonally non-stationary precipitation-runoff relationships in permafrost catchment; 4) permafrost impacts on streamflow response mostly at the beginning of the melting season; 5) allowing the temporal variations of frozen soil related parameters, i.e. the unsaturated storage capacity and the splitter of fast and slow streamflow, improved model performance. Our findings provide new insights on the impact of permafrost on catchment hydrology in vast mountain regions of western China. More generally, they help to understand the effect of climate change on permafrost hydrology.

1 Introduction

Permafrost is the ground that is at or below 0°C for at least two consecutive years. Permafrost covers 24% of the exposed land surface of the Northern Hemisphere (Zhang et al., 2005; Woo, 2012; Walwoord and Kurylyk, 2016). The high Asia region is largely covered by permafrost and is characterized by a fragile cold and arid ecosystem (Immerzeel et al., 2010; Ding et al., 2020). As this region serves as the "water tower" for nearly 1.4 billion people, understanding the permafrost hydrology is important for regional and downstream water resources management and ecosystem conservation. Permafrost prevents vertical water flow which often leads to saturated soil conditions in continuous permafrost, while confining subsurface flow through perennially unfrozen zones in discontinuous permafrost (Walvoord and Kurylyk, 2016). As an aquiclude layer, permafrost substantially controls surface runoff and its hydraulic connection with groundwater. The freeze–thaw cycle in the active layer significantly impacts soil water movement direction, velocity, storage capacity, and hydraulic conductivity (Bui et al., 2020; Gao et al., 2021).

Permafrost hydrology attracts increasing attention, as the cold regions, e.g. Arctic and high mountain Asia, are undergoing rapid changes (Tananaev et al., 2020). Permafrost degradation and its impact on hydrology is one of the research frontiers (Zhao et al., 2020; Ding et al., 2020). The question "How will cold region runoff and groundwater change in a warmer climate (e.g. permafrost thaw)?" was identified by the International Association of Hydrological Sciences (IAHS), as one of the 23 major unsolved scientific problems (Blöschl et al., 2019), which requires stronger harmonisation of community efforts. Permafrost thawing also poses great threats to the release of frozen carbon in both high altitude and latitude regions, which is likely to create substantial impacts on the climate system (Wang et al., 2020). Attention is also growing on the impacts of permafrost hydrology on nutrient transport and organic matter, and permafrost–climate feedback (Tananaev et al., 2020). Hence, there are strong motivations to understand permafrost hydrological processes (Bring et al., 2016).

Knowledge on permafrost hydrology was acquired through detailed investigations at isolated locations over various time spans by hydrologists and geocryologists (Woo et al., 2012; Gao et al., 2021). At the core scale, there are many measurements of soil profiles, including but not limited to soil temperature (Kurylyk et al., 2016; Han et al., 2018), soil moisture (Dobinski, 2011; Chang et al., 2015), groundwater fluctuation (Ma et al., 2017; Chiasson-Poirier et al., 2020), and active layer seasonal freeze-thaw processes (Wang et al., 2016; Farquharson et al., 2019). Boreholes monitor deep-soil vertical profiles, which helps to identify the distribution of permafrost and ground ice, and their dynamics (Sun et al., 2019; Ran et al., 2020). At the plot/hillslope scale, land surface energy and water fluxes are measured by eddy covariance, large aperture scintillometer (LAS), lysimeter, and multi-layers meteorological measurements. Geophysical detection technology allows us to measure various subsurface permafrost features. For example, liquid water in frozen soil can be measured by time-domain reflectometry (TDR). Ground-penetrating radar can detect the depths of the active layer and permafrost ice layer (Wu et al., 2005; Pan et al., 2017; Sokolov et al., 2020). At the basin scale, except for traditional water level and runoff gauging, water sampling and the measurements of isotopes and chemistry components provide important complementary data to understand catchment scale hydrological processes (Streletskiy et al., 2015; Ma et al., 2017; Yang et al., 2019). Remote sensing technology, including optical, near- and thermal-infrared, passive and active microwave remote sensing, has been used to identify surface landscape features (e.g. vegetation and snow cover) and directly or indirectly retrieve subsurface variables (e.g. near-surface soil freeze/thaw and permafrost state) in permafrost regions (Nitze et al., 2018; Jiang et al., 2020).

There has been a revival in the development of permafrost hydrological models simulating coupled heat and water transfer. Such models are typically physically-based and calculate seasonal freeze–thaw through solving heat transfer equations. Such equations are either solved analytically or numerically (Walvoord and Kurylyk, 2016). The Stefen equation is a typical example of the analytical approach, which calculates the depth from the ground surface to the thawing (freezing) by the integral of ground surface temperature and a thawing (freezing) index. The Stefen equation is widely used to estimate active layer thickness (Zhang et al., 2005), and is incorporated into some hydrological models (Wang L, 2010; Fabre et al. 2017). The numerical solution schemes (e.g., finite difference, finite element, or finite volume) to model ground freezing and thawing, is typically applied to one-dimensional infiltration into frozen soils, and is included in models such as SHAW (Liu et al., 2013), CoupModel (Zhou et al., 2013), the distributed water-heat coupled (DWHC) model (Chen et al. 2018), the distributed ecohydrological model (GBEHM) (Wang Y. 2018), and the three-dimensional SUTRA model (Evans et al. 2018). Andresen et al (2020) compared 8 permafrost models on soil moisture and hydrology projection across the major Arctic river basins, and found that most models project a long-term drying of surface soil, but the projection vary strongly in magnitude and spatial pattern. Except for hydrological models, many land surface models explicitly consider the freeze-thaw process, in order to improve land surface water and energy budget estimation and weather forecasting accuracy in permafrost areas. Such models include VIC (Cuo et al., 2015), JULES (Chadburn et al., 2015), CLM (Niu et al., 2006; Oleson et al., 2013; Gao et al., 2019), CoLM (Xiao et al., 2013), Noah-MP (Li et al., 2020), ORCHIDEE (Gouttevin et al., 2012). Comprehensive reviews on permafrost hydrological models can be found in Walwoord and Kurylyk (2016), Jiang et al.

(2020), and Gao et al. (2021). Model selection recommendations can be found in Bui et al (2020).

Although there are many permafrost hydrological models, most models have strong prior assumptions on permafrost hydrological behavior and therefore on its impact on catchment hydrology (Walvoord and Kurylyk, 2016; Gao et al., 2021). Such models follow a "bottom-up" modeling approach, which presents an "upward" or "reductionist" philosophy, based on the aggregation of small-scale processes and *a priori* perceptions (Jarvis, 1993; Sivapalan et al., 2003). For example, most models concentrated on estimating the heat flux from surface to deep ground. However, it is still worthwhile to note that there are unresolved questions in upscaling small scale theories on models, which does not guarantee that such models are reflective of the integrated catchment behavior. In particular, we argue that the impact of local scale freeze-thaw process on runoff should be regarded as a hypothesis to be confirmed or rejected, rather than as an assumption.

The representation of permafrost hydrological processes at the catchment scale is still controversial. Upscaling water and energy fluxes remains challenging (Muster et al., 2012; Jiang et al., 2020). Most of the process understanding was obtained from in-situ observation and modeling, which have limited spatial and invariably limited temporal coverage (Brutsaert, and Hiyama, 2012). In the headwaters of the Yellow River, some modeling studies concluded that permafrost has significant impact on streamflow (Sun et al., 2020). But in Sweden and the northeast of the United States, other studies found permafrost has negligible impact on streamflow (Shanley and Chalmers, 1999; Lindstrom et al., 2002). Some studies found that permafrost impact on streamflow is concentrated in certain periods. For example, Osuch et al. (2019) found permafrost to impact on groundwater recession and storage capacity of an active layer in Svalbard island; Nyberg et al. (2001) found that in the Vindeln Research Forest in northern Sweden permafrost impacted streamflow only in springs. Hence the link between spot scale permafrost observation, and large-scale hydrological response is still largely unknown.

The hydrograph, as an integrated signal representing catchment hydrological processes, reflects how a drainage basin transforms precipitation into runoff, and embodies the influence of basin characteristics including the geology, soils, morphology, and vegetation (Blume et al., 2007). Hence, the quantitative description of hydrographs is a valuable tool for understanding the mechanisms by which the drainage basin controls rainfall-runoff processes (McNamara et al., 1998). Diagnosing permafrost impact on catchment hydrology by analyzing the hydrograph is a promising method. For example, Slaughter and Kane (1976) found that basins with permafrost have higher peak flows and lower baseflows. Ye et al. (2008) used the peak flow/baseflow ratio to quantify the impact of permafrost coverage on hydrograph regime, and diagnosed the impact of climate change on permafrost hydrology. Moreover, the baseflow hydrography, representing groundwater recession, provides important information about the storage capacity and recession characteristics of geology, soil, and topography (Brutsaert, and Hiyama, 2012; Fenicia et al., 2008).

Using a hydrological model in small-catchment scale as a diagnostic tool is essential to understand the link between spot and large-scale hydrology (Watson et al., 2013). Although

https://doi.org/10.5194/hess-2021-264
Preprint. Discussion started: 25 May 2021

Hydrology and Earth System Sciences
Discussions

many model parameters cannot be directly observed at the catchment scale, their calibrated values and temporal dynamics provide essential information on how a catchment behaves during the precipitation-runoff process, and the roles of catchment features (geology, soil, and vegetation etc) during this process. Osuch et al. (2019) used the HBV model to diagnose the impact of permafrost on model parameter dynamics. Krogh et al. (2017) diagnosed the hydrology of a small Arctic basin in northern Canada at the tundra-taiga transition using a physically based hydrological model.

However, there is still a large lack of systematic studies linking field measurements and model experiments to understand permafrost hydrology, which is especially true for the high-altitude western China, due to the lack of long-term observations as a result of the difficulty to access and expensive to operate. The permafrost region in western China is characterized by relatively thin and warm permafrost with low ice content, due to the unique environmental conditions, arid climate, high elevation and steep geothermal gradient (Zhao et al., 2020; Jiang et al., 2020). Snow cover is much thinner than in Arctic regions, which limits the isolation effect on freeze-thaw processes. Topographical features, including aspect and elevation, are major factors affecting permafrost distribution. Complex mountainous terrain, as a result of neotectonic movement, leads to large spatial heterogeneities of energy and water balance, and underexplored permafrost hydrology in mountainous western China (Gao et al., 2021).

In this study, we utilized a top-down approach (Sivapalan et al., 2003), to understand the impacts of permafrost on catchment hydrology. We used a series of hydrological models as tools to diagnose which components play dominant roles controlling permafrost hydrology. We asked the following scientific questions:

1) Are topography and landscape important controls on streamflow generation in permafrost catchments?

2) Is permafrost groundwater recession the same as in a non-permafrost catchment? Can it be modeled by a linear reservoir?

3) Can time varying of model parameters help identifying the impacts of thawing-freezing process on catchment hydrology in permafrost regions?

These questions are addressed through a stepwise model development approach (Fenicia et al., 2008; Gao et al., 2020). We started from a simple lumped hydrological model (FLEX-L), stepwise increased complexity involving elevation distribution (FLEX-D) and landscape heterogeneity (FLEX-Topo).

As a model diagnostic tool we used dynamic identifiability analysis (DYNIA) to identify parameter dynamics. Analyzing parameter dynamics allows us to identify the temporal change of hydrological behaviors. In the end, we allowed certain parameters to be temporal dynamic, and tested whether allowing parameter dynamics could improve model performance. We believe this study deepens our understanding of permafrost hydrology, and provides new insights for future model development.

https://doi.org/10.5194/hess-2021-264
Preprint. Discussion started: 25 May 2021

2 Study site and data

The Hulu catchment (38°12´–38°17´ N, 99°50´–99°54´E) is located in the upper reaches of the Heihe River basin, the northeast edge of the Qinghai-Tibet Plateau (QTP) in Northwest China. The elevation ranges from 2960 to 4820 m a.s.l., with a span of 1860 m, and it gradually increases from north to south (Figure 1) (Chen et al., 2014; Han et al., 2018). Most precipitation happens in the summer monsoon time, and winter snowfall is low (Han et al., 2018; Jiang et al., 2020). There is a runoff gauging station at the outlet, controlling an area of 23.1 km^2. Two minor tributaries are sourced from glaciers (east) and moraine–talus (west) zones and then merge at the catchment outlet. The Hulu catchment has rugged terrain and little human disturbance. The Hulu catchment mostly extends on permafrost (Zou et al., 2014). We identified four main landscape types, i.e. glaciers (5.6%), alpine desert (53.5%), vegetation hillslope (37.5%), and riparian zone (3.4%) (Figure 1).

We used daily runoff data, 2m daily average air temperature and daily precipitation data from January 1st 2011 to December 31st 2014 in this study. The elevation of the hydrometeorological gauging station is 2980m. There was a big flood event in 2013, which damaged the water level sensor, which caused a runoff data gap from June 17th to July 10th in 2013. Soil moisture was measured in 20cm, 40cm, 80cm, 120cm, 180cm, 240cm, and 300cm depths from October 1st 2011 to December 31st 2013, with a data gap between August 3rd 2012 and October 2nd 2012. Groundwater depth was measured at two locations, i.e. WW01 and WW03, from June 25th 2014 to September 17th 2016. WW01 has 4 wells with depths of 5m, 10m, 15m and 25m; and WW03 has 2 wells, with depths of 20m and 30m.

3 Modelling approach

In the following, we describe the 3 model structures (Sections 3.1, 3.2, and 3.3), as well as the uncertainty analysis, evaluation functions and calibration framework in Section 3.4. In Section 3.5, the dynamic identifiability analysis (DYNIA) was introduced to diagnose the temporal variation of parameters.

3.1 FLEX-L model

The FLEX-L is a lumped hydrological model (Fenicia et al., 2011; Gao et al., 2014), with four reservoirs, i.e. the snow reservoir (S_w), unsaturated reservoir (S_u), the fast response reservoir (S_f), and the groundwater reservoir (S_s). There are 8 parameters in the FLEX-L, including the snow degree-day factor (F_{dd}), the storage capacity of the unsaturated reservoir (S_{umax}), the threshold value controlling evaporation (C_e), the shape parameter of the unsaturated reservoir (β), the splitter between fast response reservoir and slow response (baseflow) reservoir (D), the recession parameter of faster reservoir (K_f), the recession parameter of baseflow reservoir (K_s), and lag time from rainfall event to peak flow (T_{lagF}). We set prior ranges for the parameters based on previous studies (Gao et al., 2014; Gao et al., 2020), i.e.

F_{dd} (1-5), S_{umax} (1-150), C_e (0-1), β (0-1), D (0-1), K_f (1-10), K_s (9-100), and T_{lagF} (0.8-2). Due to shallow and ephemeral snow cover in this region, we used simple snow accumulation and melting module to limit the number of free parameters.

3.2 FLEX-D model

The FLEX-D is a distributed hydrological model (Gao et al., 2014), developed based on the FLEX-L, with the same parameters as FLEX-L, but distributed inputs. The Hulu catchment (from 2960m to 4820m) was classified into 37 elevation bands, with 50m interval. We interpolated the precipitation and temperature based on elevation bands from in-situ observation (2980m) to each elevation band. The precipitation increase rate was set as 4.2%/100m, and temperature lapse rate as 0.68°C/100m, based on field measurement (Han et al., 2013). FLEX-D uses the same model structure and parameter set in each elevation band. The model structures run in parallel and the corresponding discharge is subsequently aggregated.

3.3 FLEX-Topo model

The structure of FLEX-Topo model consists of four parallel components, representing the distinct hydrological function of different landscape elements (Savenije, 2010; Gao et al., 2014; Gharari et al., 2014; Gao et al., 2016). We classified the entire Hulu catchment into four landscapes, i.e. glaciers, alpine desert, vegetation hillslope, and riparian zone. Combined with 37 elevation bands, we have 37×4=148 landscape elements.

For glaciers, we used a temperature-index glacio-hydrological module to simulate the glacier melting (Gao et al., 2020). We kept the model structure for vegetation hillslope, riparian and alpine desert the same as FLEX-L, and gave different unsaturated storage capacity (S_{umax}) values for different landscapes, i.e. S_{umax_R} for riparian, S_{umax_D} for cold desert, and S_{umax_V} for hillslope vegetation.

For vegetation hillslope, we constrained a larger prior range for the unsaturated storage capacity (S_{umax_V}) (10~200mm), which means more water is needed to fill in its storage capacity to meet its water deficit, which is evidenced by previous studies in this region (Gao et al., 2014). For alpine desert, due to its sparse vegetation cover, we constrained a shallower unsaturated storage capacity (S_{umax_D}) (1~150mm). For riparian area, due to its location which is prone to be saturated, we also constrained a shallower unsaturated storage capacity (S_{umax_R}) (1~150mm).

3.4 Model uncertainty analysis and evaluation functions

The Kling-Gupta efficiency (Gupta et al., 2009; KGE) was used as the performance metric in model calibration:

https://doi.org/10.5194/hess-2021-264
Preprint. Discussion started: 25 May 2021

Hydrology and Earth System Sciences
Open Access
Discussions

$$KGE = 1 - \sqrt{(r-1)^2 + (\alpha-1)^2 + (\beta-1)^2} \quad (1)$$

Where r is the linear correlation coefficient between simulation and observation; α ($\alpha = \sigma_m/\sigma_o$) is a measure of relative variability in the simulated and observed values, where σ_m is the standard deviation of simulated variables, and σ_o is the standard deviation of observed variables; β is the ratio between the average value of simulated and observed variables.

We applied the Generalized Likelihood Uncertainty Estimation framework (GLUE, Beven and Binley, 1992) to estimate model parameter uncertainty. Sampling the parameter space with 20, 000 parameter sets, and select the top 1% parameter as behavioral parameter sets.

For a comprehensive assessment of model performance in validation, the behavioral model runs were evaluated using multiple criteria, including KGE, KGL (the KGE of logarithms flow, and more sensitive to baseflow), Nash-Sutcliffe Efficiency (NSE) (Nash and Sutcliffe, 1970) (Equation 2), coefficient of determination (R^2) and root mean square error (RMSE).

$$NSE = 1 - \frac{\sum_{t=1}^{n}(Q_o - Q_m)^2}{\sum_{t=1}^{n}(Q_o - \overline{Q_o})^2} \quad (2)$$

Where Q_o is observed runoff, $\overline{Q_o}$ is the observed average runoff, and Q_m is modeled runoff.

The model was calibrated in the period 2011-2012, and KGE as objective function. The second half time series (2013-2014) were used to quantify the model performance in streamflow split-sample validation, with multi-criteria including KGE, KGL, NSE, R^2, and RMSE.

3.5 DYNIA algorithm

The dynamic identifiability analysis (DYNIA) (Wagener et al., 2003; Pianosi and Wagener, 2016) is an approach to diagnose the temporal variation of parameters. It is based on the GLUE approach, but evaluated on a moving time window. DYNIA allows to assess how the conditional marginal cumulative distribution function for each parameter varies with time. This analysis allows to identify the periods where conditioning takes place on individual model parameters (i.e. where data is informative or not). Conceptual model parameters, although not measurable quantities, are associated to specific process representations (Fenicia et al., 2009). Hence the variability of parameters can represent the catchment properties change over time. In the case of this study, we focus our attention to permafrost related parameters and associated processes.

The chosen window size allows for tailoring across influence scales of parameters. In this study, a moving window with non-overlapping 10-days length was applied (Osuch, 2019). The same threshold as with the application of the GLUE approach was applied. Hence, we selected the top 1% parameter as behavioral parameter sets for each time window.

https://doi.org/10.5194/hess-2021-264
Preprint. Discussion started: 25 May 2021

4 Experiments design

4.1 Testing the importance of distributed forcing and landscape heterogeneity (Exp1-Exp4)

Exp 1: lumped model FLEX-L with observed meteorology data at 2980m as input. This experiment uses the data measured at the meteorological gauging station as model inputs.

Exp 2: lumped model FLEX-L with corrected meteorology data by topography as input. This experiment averages the distributed meteorological forcing data as described in Section 3.2 as model inputs.

Exp 3: distributed model FLEX-D with distributed meteorology data as input. This experiment uses a distributed model based on elevation zones, and uses the distributed data described in Section 3.2 in each elevation zone.

Exp 4: landscape-based FLEX-Topo model, with landscape heterogeneity and driven by distributed meteorological data the same as FLEX-D.

The models are calibrated and validated as described in Section 3.4.

4.2 Groundwater analysis (Exp5)

Baseflow recession provides an important source of information to infer groundwater characteristic, including its storage properties, subsurface hydraulics, and concentration times (Brutsaert and Sugita, 2008; Fenicia et al., 2006). Especially for permafrost basins, the freeze-thaw process is thought to have significant impact on baseflow recession. Thus, the recession curve provides an instrument to identify the impact of permafrost on streamflow (Ye et al., 2009).

Baseflow analysis is based on the water balance equation (Equation 3), and linear reservoir assumption (Equation 4). If a reservoir is linear, this means that the reservoir discharge (Q) has a linear relationship with storage (S). K_S (days) is a time-constant controlling the speed of recession. With a larger K_S value, reservoir recedes slower, and vise versa. Combining Equation 3 and 4, we can derive equation 5, illustrating how discharge depends on time. Brutsaert and Sugita (2008) proposed an alternative relationship to derive the recession constant from data (Equation 6). Based on these equations, we can analyses permafrost groundwater characteristic by the performance of this linear recession model, and the value of K_S.

$$\frac{dS}{dt} = -Q \quad (3)$$

$$Q = S/Ks \quad (4)$$

https://doi.org/10.5194/hess-2021-264
Preprint. Discussion started: 25 May 2021

Hydrology and Earth System Sciences
Discussions
Open Access
EGU

$$Q = Q_0 \cdot e^{-t/Ks} \quad (5)$$

$$Q = Ks \cdot \frac{dQ}{dt} \quad (6)$$

K_s was obtained by curve-fitting, and set as a constant in Exp5 and the following experiments. Calibration and validation methods were kept the same as Exp1-4.

4.3 Identify parameter variation (Exp6-10)

We firstly applied DYNIA approach to obtain the temporal variations of all 11 parameters from 2011 to 2014. Then to evaluate the impacts of parameter variations on model performance, from Exp6 to Exp10, we allowed different parameters as temporal variation which were obtained by DYNIA, while setting the other parameters as time-invariant to be calibrated. We tested the impacts of parameter variations on model performance in validation (2013-2014), with multi-criteria, including KGE, NSE, KGL, R^2, and RMSE.

Exp6: we set the snow and glacier related parameters (F_{dd}, F_{ddG}) as temporally varying, and other parameters as time-invariant, and test their impact on model performance in validation;

Exp7: we set the runoff generation related parameters (S_{umax_R}, S_{umax_V}, S_{umax_D}, β, C_e) as dynamic, and other parameters as time-invariant, and test their impact on model performance in validation;

Exp8: we set the response related parameters (K_s, K_f, D, T_{lagF}) as dynamic, and other parameters as time-invariant, and test their impact on model performance in validation;

Exp9: we set all parameters as dynamic, and test their impact on model performance in validation;

Exp10: based on an assessment of how model parameters are intended to affect modeled processes, we allowed 3 parameters to vary, namely D, S_{umax_V}, S_{umax_D}, and other parameters as time-invariant. We allowed D to vary, because permafrost is a barrier to groundwater recharge, freeze-thaw process strongly impacts the connection between soil and groundwater, and the value of D (Sjöberg et al., 2013). S_{umax_V}, S_{umax_D} are the parameters controlling storage capacity of unsaturated reservoir, which are very likely linked with the active layer depth.

https://doi.org/10.5194/hess-2021-264
Preprint. Discussion started: 25 May 2021

5 Results

5.1 Accounting for topography and landscape in model structure (Exp1-4)

Exp 1 to Exp 3 are intended to test the impact of different meteorological forcings on model results. Exp 1 resulted in the following streamflow performance metrics: in calibration KGE=0.57; in validation, KGE=0.35, KGL= -0.21, NSE= -0.02, R^2= 0.67, and RMSE= 1.35mm (Figure 4). In Exp1, merely from analysis of the observed data, we found that the total runoff is 499mm/a, which is even larger than observed precipitation 433mm/a. This means that the runoff coefficient is larger than 1, and the water balance cannot be closed with the current setup. This explains the relatively low value of the performance indicators. The high value of the runoff coefficient was explained assuming that precipitation is strongly underestimated, especially in high elevation zones (Han et al., 2017, Zhao et al., 2020).

In Exp2, we kept the FLEX-L model structure, but corrected the meteorology forcing accounting for elevation. The precipitation increase rate was set as 4.2%/100m, and temperature lapse rate was 0.68°C/100m (Han et al., 2013). Precipitation correction improved model performance. KGE in calibration improved to 0.73. In validation, KGE = 0.49, KGL = 0.14, NSE = 0.05, R^2 = 0.71, and RMSE = 1.20mm.

In Exp3, we used the distributed FLEX-D model, and corrected the observed precipitation and temperature from the meteorological station (2980m) to corresponding elevation band, based on the same temperature and precipitation lapse rate as Exp2. KGE in calibration was further improved to 0.82. In validation, the KGE= 0.55, KGL =0.09, NSE= 0.22, R^2= 0.76, and RMSE was reduced to 1.09mm.

In Exp 4, the results (Figure 4) clearly showed that accounting for landscape heterogeneity improved model performance. KGE in calibration was further improved to 0.84. In validation, the KGE =0.55, KGL =0.19, NSE =0.29, R^2= 0.80, and RMSE= 1.04mm. The FLEX-Topo model estimated that glaciers only covers 5.6% area, but contributes 19% runoff; vegetation hillslope covers 37.5% area, but only contributes 20.1% runoff; alpine desert covers 53.5%, and contributes 58.7% runoff; riparian area covers 3.4% area, and contributes 2.3% runoff. These results are largely in line with field-obtained expert knowledge. These results manifest the importance of considering landscape heterogeneity in models to accurately simulate the spatial diversity of hydrological processes in permafrost regions.

5.2 Permafrost recession analysis (Exp5)

In Figure 6, we plot the groundwater recession on logarithmic scale, and found a clear linear recession curve. When we set the K_s at 80 days, the linear reservoir model can fit all four years' recession. We also plot the Q vs dQ/dt. The K_s =80d also well represent the

https://doi.org/10.5194/hess-2021-264
Preprint. Discussion started: 25 May 2021

observations (Figure 7).

With respect to the parameterization of the reservoir that simulates the slow hydrograph component, we determined that in general a linear model can well represent the groundwater behavior of the catchments. With fixed K_s as 80 days, we did Exp 5. And the model performance for KGE was 0.82. In validation, the KGE = 0.57, KGL was significantly improved to 0.73 (0.19 in Exp4), NSE =0.26, R^2 =0.78, and RMSE= 1.06. In the following experiments, we fixed the K_s as 80 d.

5.3 Using dynamic parameters to infer permafrost processes (Exp6-10)

In Exp6, we allowed the snow and glacier melt related parameters (F_{dd} and F_{ddG}) to be dynamic as obtained by DYNIA, and fixed the other parameters as time-invariant. In model validation, the KGE improves to 0.61, KGL =0.65, NSE= 0.28, R^2 =0.76, and RMSE= 1.05mm. Comparing with Exp5, KGE is improved from 0.57 to 0.61, and KGL was slightly decreased from 0.73 to 0.65 likely because of the random uncertainty caused by snow/glacier melting parameter dynamic.

In Exp 7, the unsaturated reservoir parameters (S_{umax_R}, S_{umax_V}, S_{umax_D}, β, C_e) were allowed to be temporally dynamic, and kept other parameters as time-invariant. In this experiment, the KGE =0.60, KGL= 0.63, NSE= 0.36, R^2 =0.80, and RMSE= 0.99mm. Compared with Exp6, the NSE was improved, and other criteria did not change significantly.

In Exp 8, the response related parameters (K_s, K_f, D, T_{lagF}) were allowed to be temporally dynamic. In this experiment, all criteria were improved comparing with Exp7. the KGE was increased to 0.75, KGL =0.70, NSE =0.59, R^2 =0.84, and RMSE was reduced to 0.79mm. Model improvement in Exp8 indicates response routine has much temporal variation and seasonality. Further investigation on the impact of permafrost on response routine, probably related to hydrological connectivity, will likely improve model performance.

In Exp 9, all the parameters were allowed to be dynamic. And we obtained the best model performance in validation in this study, the KGE =0.86, KGL =0.66, NSE= 0.75, R^2= 0.88, and RMSE= 0.62mm. The DYNIA results clearly shows the impact of permafrost on hydrological processes, but mostly in the beginning of melting season.

In order to test the key parameters on model performance, we allow three key parameters (D, S_{umax_V}, S_{umax_D}) to be dynamic in Exp 10. The results are not much different with Exp9: KGE =0.84, KGL= 0.70, NSE= 0.73, R^2= 0.87, and RMSE= 0.64mm. This result confirmed our hypothesis that these parameters are important to determine performance. Also allowing a smaller number of free dynamic parameters can have a much clearer parameter dynamic pattern.

Summarily, Figure 8 shows that while allowing snow and ice parameter to have temporal variation, there is little improvement. And allowing for runoff generation and response routine parameters variation resulted in more significant improvements. These results indicate, we should pay more attention to runoff generation and runoff response to understand the impacts of permafrost on hydrology.

Interestingly, only allowing three parameters to be dynamic, including S_{umax_V}, S_{umax_D}, and D, has similar results as all parameters' dynamic in Exp9. In further studies, we should develop new parameterization to make more physical connection between S_{umax_V}, S_{umax_D}, D and permafrost impacts. We argue that clarifying which processes are more important than others, and the selection of involving certain processes, and neglecting certain processes may be more important than accurately solving differential equations (Savenije, 2009).

6 Discussion

6.1 Using stepwise modeling to understand hydrology

The results of Exp1-3 demonstrate the importance of correct forcing input for model performance. Without correcting precipitation for elevation, we cannot even close the water balance, and the simulation cannot be right. This result is also in line with previous studies, showing that precipitation in mountainous areas is largely underestimated (Immerzeel et al., 2015; Chen et al., 2018; Zhang et al., 2018b).

It is worthwhile to note that the large model errors are manifested in the beginning of the melting seasons for all 4 years simulation for FLEX-L and FLEX-D models in Exp1-3 (Figure 5). The two models significantly overestimated runoff in the beginning of the melting seasons. After explicitly considering landscape heterogeneity in Exp4, the performance of the FLEX-Topo model was improved, likely due to the inclusion of the following processes: in the beginning of the melting season, snow starts to melt in low elevations, which has good vegetation cover and large rootzone storage capacity. The melt water firstly fills in the water deficit in the large rootzone storage capacity on the vegetated hillslope, without much runoff generation. Hence, considering landscape heterogeneity reduced model discrepancy. However, the overestimation of runoff in the beginning of the melting season still exists, which we hypothesize to be impacted by permafrost and will be discussed in Section 6.3.

From stepwise model comparison, we learned that involving topography and landscape is important to reproduce streamflow. Moreover, we found that even without the explicit consideration of permafrost impacts, the FLEX-Topo model can reproduce hydrographs in dominant periods. This is in line with most studies showing that permafrost does not have significant impacts on the total amount of runoff generation, but influences hydrological processes in certain periods (Fabre et al., 2017; Osuch et al., 2019).

https://doi.org/10.5194/hess-2021-264
Preprint. Discussion started: 25 May 2021

6.2 Baseflow recession in permafrost regions

Only from the shape of the curves in Figure 6 and 7, we did not find significant differences between this permafrost catchment and other regions. The linear recession seems free of influence by the surface freeze-thaw process. But the K_s parameter value (80d) is much larger than 43d in non-permafrost regions (Brutsaert and Hiyama, 2012). We credit these characteristics to the presence of permafrost. McNamara et al., (1998) also found the specific recession constant K_s in permafrost region of Alaska is higher than in non-permafrost basins. This means in a permafrost region groundwater recession is slower than in non-permafrost regions, and groundwater recession is extended by permafrost. Highly absorptive surface layers and low evaporation may explain this phenomenon (McNamara et al., 1998).

Baseflow recession was used to identify the impacts of climate change on permafrost and catchment hydrology. For example, an increase in yearly minimum discharges was detected using streamflow characteristics to explore permafrost thawing in northern Swedish catchments (SjöBerg et al., 2013). Trends of increasing baseflow have also been observed in Arctic Russia (Smith et al. 2007), the Yukon River in Alaska (USA) (StJacques and Sauchyn 2009; Walvoord and Striegl 2007), the Lena River in Russia (Ye et al. 2009), the whole pan-Arctic (Rennermalm et al. 2010), and Western China (Niu et al., 2010), for varying time periods covering the last century and the beginning of this century. Long-term trends in recession flows, as a proxy for permafrost thaw, have been analyzed in northern Sweden (Lyon et al. 2009) and the Yukon River basin (Lyon and Destouni 2010). Lyon et al. (2009) estimated that permafrost in a sub-arctic catchment was thawing at an average rate of about 0.9 cm/yr during the past 90 years, which was consistent with direct observation of permafrost thawing rate. This means hydrography itself provides useful information to understand the impact of permafrost on streamflow, and confirms the feasibility of using hydrologic observations to infer changes in catchment scale permafrost.

6.3 Model parameters dynamics and permafrost hydrological connectivity

Figure 9 demonstrates the temporal variation of three model parameters (S_{umax_D}, S_{umax_V}, D). We found that considering the temporal variation of these parameters, model performance was improved, especially for the beginning of melting season in all four years simulation. We also plot parameters dynamics with multi physical variables in Figure 10, including groundwater depth, soil moisture of different layers, soil temperature in different layers, frozen depth and hydrograph simulation, highlighting the beginning of the melting season. Figure 9 shows S_{umax_V}, S_{umax_D} had larger values in this period, indicating that the unsaturated soil has larger volume storage capacity in these periods when soil starts to thaw but still with frozen soil in the bottom of the active layer (Figure 10). D is smaller in the beginning of the melting season and the end of the melting season (i.e. the recession periods), indicating the infiltrated water in these two periods is mostly stored in supra-permafrost soil, due to the frozen bottom of the active layer. In the middle of the melting season, *D* is large, indicating the connectivity between surface and groundwater systems, and that hydrological response from rainfall/snowmelt to runoff was fast. These parameter behaviors match well with the deep groundwater level measurements in 4 wells in WW01, and 2 wells in WW03, the gradual increasing of soil moisture from 20cm depth to 300cm depth, the increase of soil temperature from 0cm to 160cm, and the thawing of top frozen soil. All these phenomena occur simultaneously with very limited river runoff generation (red dash box), likely due to the initial dry soil and the increasing unsaturated soil storage capacity with the increase of soil temperature and deepening of unfrozen top soil. The existence of supra-permafrost water and the impermeability of bottom active layer, resulted in the vertical disconnection between surface and groundwater. And different landscapes caused the lateral disconnection between hillslope and river channel. With the increase of soil moisture and thawing of the active layer, the vertical and lateral connections resulted in the increase of runoff generation in the middle of the melting season. After considering parameter dynamics, Exp10 improved model performance, especially in the beginning of the melting season (Figure 8, 9, 10).

These results motivated the following perceptual model. In winter, although top soil was frozen, groundwater recession did not stop, which increased soil moisture deficit in the beginning of the melting season. Due to thin snow cover in the Hulu catchment, soil evaporation in winter also continued. After a long winter groundwater recession and soil evaporation, in the beginning of the melting season, soil became dry and deficit of moisture, and the groundwater level was deep. Thus, the unsaturated reservoir storage capacity (S_{umax_V} and S_{umax_D}) was large. That is why the precipitation during this period does not generate much runoff, since this amount of precipitation firstly infiltrates and reduces the moisture deficit. The deep groundwater, increasing soil moisture and temperature, and deepening frost boundary, form strong evidence to support this concept. Gradually, with the increase of the thawing process, soil becomes wet from top soil to deeper soil, soil moisture and temperature increases from top to bottom, the frost boundary deepens downward. Groundwater level variation observed by 4 wells in WW01 and 2 wells in WW03, show a similar phenomenon. These observations indicate the increasing of the active layer depth, and the increase of soil moisture in the beginning of the melting season. In the middle of the melting season, the active layer is thoroughly thawed, and the unsaturated soil layer becomes saturated, and the value of S_{umax_V} and S_{umax_D} is reduced, resulting in larger runoff generation.

For future studies, we recommend to pay particular attention to the hydrological processes in the beginning of the melting season. Moreover, we recommend to develop process-based models to simulate the impact of the thawing soil on the temporal variation of the unsaturated reservoir storage capacity (S_{umax_V} and S_{umax_D}), and the impact of freeze/thaw processes on hydrological connectivity between surface and groundwater (*D*).

https://doi.org/10.5194/hess-2021-264
Preprint. Discussion started: 25 May 2021

6 Conclusions

Our knowledge on permafrost hydrology in mountainous regions is still incomplete. We have collected numerous heterogeneities and complexities in permafrost regions, but most of these observations are still not well considered in catchment scale hydrological modeling. More importantly, we still largely lack knowledge on which variables play a more dominant role at certain spatial-temporal scales, and should be included in hydrological models as priority.

By conducting this study with field measurements and model experiments, we reached the following conclusions: 1) correct meteorological forcing input is essential in mountainous hydrological modeling; 2) distributed modeling based on topography and landscape is important in cold regions with complex terrain; 3) baseflow recession in permafrost region is well approximated by a linear reservoir, but the recession parameter K_s is much larger than in other regions; 4) even without explicitly involving the freeze-thaw process, the hydrological model can mimic and reproduce most parts of the hydrograph; 5) allowing parameter dynamics improved model performance, especially in the beginning of the melting season. Particular attention needs to be paid to understand and model the thawing process at the beginning of the melting season, and its impacts on hydrological connectivity at the catchment-scale. This diagnostic study benefits our understanding on permafrost hydrology from measured data rather than arbitrary prior assumptions. We believe this study is able to give us new insights into further implications to understand the impact of permafrost on hydrology, and projecting climate change on permafrost hydrology.

ACKNOWLEDGMENTS

This study was supported by the National Natural Science Foundation of China (Grant Nos. 42071081, 41801036, 4181101490, 41971041, and 41771262).

References:

Andresen, C. G., Lawrence, D. M., Wilson, C. J., McGuire, A. D., Koven, C., Schaefer, K., Jafarov, E., Peng, S., Chen, X., Gouttevin, I., Burke, E., Chadburn, S., Ji, D., Chen, G., Hayes, D., and Zhang, W.: Soil moisture and hydrology projections of the permafrost region – a model intercomparison, The Cryosphere, 14, 445–459, https://doi.org/10.5194/tc-14-445-2020, 2020.

Beven, K. and Binley, A.: The Future of Distributed Models –Model Calibration and Uncertainty Prediction, Hydrol. Process., 6, 279–298, 1992.

Blume, T., Zehe, E., Bronstert, A. (2007) Rainfall—runoff response, event-based runoff

https://doi.org/10.5194/hess-2021-264
Preprint. Discussion started: 25 May 2021

Hydrology and Earth System Sciences Discussions
Open Access

coefficients and hydrograph separation, Hydrological Sciences Journal, 52:5, 843-862, DOI: 10.1623/hysj.52.5.843

Blöschl, G., Twenty-three unsolved problems in hydrology (UPH) – a community perspective. Hydrological Sciences Journal, 2019

Bring, A., I. Fedorova, Y. Dibike, L. Hinzman, J.Mård, S. H.Mernild, T. Prowse, O. Semenova, S. L. Stuefer, andM.-K.Woo (2016), Arctic terrestrial hydrology: A synthesis of processes, regional effects, and research challenges, J. Geophys. Res. Biogeosci., 121, 621–649, doi:10.1002/2015JG003131.

Brutsaert, W.& Sugita, M. (2008) Is Mongolia's groundwater increasing or decreasing? The case of the Kherlen River basin / Les eaux souterraines de Mongolie s'accroissent ou décroissent-elles? Cas du bassin versant la Rivière Kherlen, Hydrological Sciences Journal, 53:6, 1221-1229, DOI: 10.1623/hysj.53.6.1221

Brutsaert, W., and T. Hiyama (2012), The determination of permafrost thawing trends from long-term streamflow measurements with an application in eastern Siberia, J. Geophys. Res., 117, D22110, doi:10.1029/2012JD018344.

Bui, M.T.; Lu, J.; Nie, L. A Review of Hydrological Models Applied in the Permafrost-Dominated Arctic Region. Geosciences 2020, 10, 401.

Chadburn, S., Burke, E., Essery, R., Boike, J., Langer, M., Heikenfeld, M., Cox, P., and Friedlingstein, P.: An improved representation of physical permafrost dynamics in the JULES land-surface model, Geosci. Model Dev., 8, 1493–1508, https://doi.org/10.5194/gmd-8-1493-2015, 2015.

Chang J, Wang G X, Li C J, et al. 2015. Seasonal dynamics of suprapermafrost groundwater and its response to the freeing-thawing processes of soil in the permafrost region of Qinghai-Tibet Plateau. Science China: Earth Sciences, 58: 727–738, doi: 10.1007/s11430-014-5009-y

Chen, R.S., Song, Y.X., Kang, E.S., Han, C.T., Liu, J.F., Yang, Y., Qing, W.W., &Liu, Z.W. (2014). A Cryosphere-Hydrology Observation System in a Small Alpine Watershed in the Qilian Mountains of China and Its Meteorological Gradient. Arctic, Antarctic, and Alpine Research, 46(2), 505-523.

Chen, R., Wang, G., Yang, Y., Liu, J., Han, C., Song, Y., et al. (2018a). Effects of cryospheric change on alpine hydrology: Combining a model with observations in the upper reaches of the Hei River, China. Journal of Geophysical Research: Atmospheres, 123, 3414–3442. https://doi.org/10.1002/2017JD027876

Chen, Rengsheng, Chuntan Han, Junfeng Liu, Yong Yang, Zhangwen Liu, Lei Wang, Ersi Kang; Maximum precipitation altitude on the northern flank of the Qilian Mountains, northwest China. Hydrology Research, 2018b; 49 (5): 1696–1710.

Chiasson-Poirier, G., Franssen, J. M. J., Lafrenière, D., Fortier, S. F. L., Seasonal evolution of active layer thaw depth and hillslope-stream connectivity in a permafrost watershed, Water Resources Research, 2020, 56, e2019WR025828.

Cuo, L., Zhang, Y., Bohn, T. J., Zhao, L., Li, J., Liu, Q., and Zhou, B. (2015), Frozen soil degradation and its effects on surface hydrology in the northern Tibetan Plateau, J. Geophys. Res. Atmos., 120, 8276– 8298, doi:10.1002/2015JD023193.

Ding Y, Zhang S, Chen R, Han T, Han H, Wu J, Li X, Zhao Q, Shangguan D, Yang Y, Liu J, Wang S, Qin J and Chang Y (2020) Hydrological Basis and Discipline System of Cryohydrology: From a Perspective of Cryospheric Science. Front. Earth Sci. 8:574707. doi: 10.3389/feart.2020.574707

Dobinski, W. Permafrost. Earth-Science Reviews 108 (2011) 158–169

Evans, S. G., Ge, S., Voss, C. I., and Molotch, N. P. (2018). The role of frozen soil in groundwater discharge predictions for warming alpine watersheds. Water Resour. Res. 54, 1599–1615. doi:10.1002/2017WR022098

Fabre, C. Using Modeling Tools to Better Understand Permafrost Hydrology. Water, 2017, 9, 418; doi:10.3390/w9060418

Farquharson, L. M., Romanovsky, V. E., Cable, W. L., Walker, D. A., Kokelj, S. V., & Nicolsky, D. (2019). Climate change drives widespread and rapid thermokarst development in very cold permafrost in the Canadian High Arctic. Geophysical Research Letters, 46, 6681–6689. https://doi.org/10.1029/2019GL082187

Fenicia, F. Is the groundwater reservoir linear? Learning from data in hydrological modelling. Hydrol. Earth Syst. Sci., 10, 139–150, 2006

Fenicia, F., H. H. G. Savenije, P. Matgen, and L. Pfister (2008), Understanding catchment behavior through stepwise model concept improvement, Water Resour. Res., 44, W01402, doi:10.1029/2006WR005563.

Fenicia, F., Savenije, H. H. G., and Avdeeva, Y.: Anomaly in the rainfall-runoff behaviour of the Meuse catchment. Climate, land-use, or land-use management?, Hydrol. Earth Syst. Sci., 13, 1727–1737, https://doi.org/10.5194/hess-13-1727-2009, 2009.

Fenicia, F., Kavetski, D., Savenije, H.H.G., 2011. Elements of a flexible approach for conceptual hydrological modeling: 1. Motivation and theoretical development. Water Resour. Res. 47. https://doi.org/10.1029/2010wr010174.

Gao, B. , Yang, D. , Qin, Y. , Wang, Y. , Li, H. , & Zhang, Y. , et al. (2018). Change in frozen soils and its effect on regional hydrology, upper heihe basin, northeastern qinghai-tibetan plateau. Cryosphere, 12(8), 657-673.

Gao, H., Hrachowitz, M., Fenicia, F., Gharari, S. & H.H.G. Savenije (2014). Testing the realism of a topography-driven model (FLEX-Topo) in the nested catchments of the upper Heihe, China. Hydrology and Earth System Sciences 18: 1895-1915.

Gao, H., M. Hrachowitz, N. Sriwongsitanon, F. Fenicia, S. Gharari, and H. H. G. Savenije (2016), Accounting for the influence of vegetation and landscape improves model transferability in a tropical savannah region, Water Resour. Res., 52, doi:10.1002/2016WR019574.

https://doi.org/10.5194/hess-2021-264
Preprint. Discussion started: 25 May 2021

Gao, H., Ding, Y., Zhao, Q., Hrachowitz, M., Savenije, H.H.G., 2017a. The importance of aspect for modelling the hydrological response in a glacier catchment in Central Asia. Hydrol. Process. 31 (16), 2842–2859. https://doi.org/10.1002/hyp.11224.

Gao, H., Dong, J., Chen, X., Cai, H., Liu, Z., Jin, Z., Mao, D., Yang, Z., Duan, Z. (2020). Stepwise modeling and the importance of internal variables validation to test model realism in a data scarce glacier basin. Journal of Hydrology. 591, 125457

Gao, H. (2021) Permafrost hydrology of the Qinghai-Tibet Plateau: A review of processes and modeling. Front. Earth Sci. | doi: 10.3389/feart.2020.576838

Gao, J., Xie, Z., Wang, A., Liu, S., Zeng, Y., Liu, B., et al. (2019). A new frozen soil parameterization including frost and thaw fronts in the Community Land Model. Journal of Advances in Modeling Earth Systems, 11, 659– 679

Gharari, S., Hrachowitz, M., Fenicia, F., Gao, H., and Savenije, H. H. G.: Using expert knowledge to increase realism in environmental system models can dramatically reduce the need for calibration, Hydrol. Earth Syst. Sci., 18, 4839–4859, https://doi.org/10.5194/hess-18-4839-2014, 2014.

Gouttevin, I., Krinner, G., Ciais, P., Polcher, J., and Legout, C. (2012). Multi-scale validation of a new soil freezing scheme for a land-surface model with physically-based hydrology. Cryosphere 6, 407–430. doi:10.5194/tc-6-407-2012

Gupta, H. V., Kling, H., Yilmaz, K. K., and Martinez, G. F.: Decomposition of the mean squared error and nse performance criteria: Implications for improving hydrological modelling, Journal of Hydrology, 377, 80-91, http://dx.doi.org/10.1016/j.jhydrol.2009.08.003, 2009.

Han, C., Chen, R., Liu, J., Yang, Y., Liu, Z. (2013). Hydrological characteristics in non-freezing period at the alpine desert zone of Hulugou watershed, Qilian Mountains. Journal of Glaciology and Geocryology, 2013, 35(6): 1536-1544.

Han, C., R. Chen, Z. Liu, Y. Yang, J. Liu, Y. Song, L. Wang, G. Liu, S. Guo, and X. Wang. 2018. Cryospheric Hydrometeorology Observation in the Hulu Catchment (CHOICE), Qilian Mountains, China. Vadose Zone J. 17:180058. doi:10.2136/vzj2018.03.0058

Hülsmann, L., Geyer, T., Schweitzer, C. et al. The effect of subarctic conditions on water resources: initial results and limitations of the SWAT model applied to the Kharaa River Basin in Northern Mongolia. Environ Earth Sci 73, 581–592 (2015).

Immerzeel, W. W., Van Beek, L. P. H., and Bierkens, M. F. P. (2010). Climate change will affect the asian water towers. Science. 328, 1382–1385. doi:10.1126/science.1183188

Immerzeel, W.W., Wanders, N., Lutz, A.F., Shea, J.M., Bierkens, M.F.P., 2015. Reconciling high-altitude precipitation in the upper Indus basin with glacier mass balances and runoff. Hydrol. Earth Syst. Sci. 19, 4673–4687. https://doi.org/10.5194/hess-19-4673-2015.

Jarvis PG. 1993. Prospects for bottom-up models. In Scaling Physiological Processes: Leaf to Globe. Ehleringer JR, Field CB (eds). Academic Press.

Jiang H, Zheng G, Yi Y, Chen D, Zhang W, Yang K and Miller CE (2020) Progress and

https://doi.org/10.5194/hess-2021-264
Preprint. Discussion started: 25 May 2021

Challenges in Studying Regional Permafrost in the Tibetan Plateau Using Satellite Remote Sensing and Models. Front. Earth Sci. 8:560403. doi: 10.3389/feart.2020.560403

Krogh, S., Pomeroy, J. W., Marsh, P. Diagnosis of the hydrology of a small Arctic basin at the tundra-taiga transition using a physically based hydrological model. Journal of Hydrology 550 (2017) 685–703

Kurylyk, B. L., M. Hayashi, W. L. Quinton, J. M. McKenzie, and C. I. Voss (2016), Influence of vertical and lateral heat transfer on permafrost thaw, peatland landscape transition, and groundwater flow, Water Resour. Res., 52, 1286–1305, doi:10.1002/2015WR018057.

Li, X., Wu, T., Zhu, X., Jiang, Y., Hu, G., & Hao, J., et al. (2020). Improving the Noah-MP model for simulating hydrothermal regime of the active layer in the permafrost regions of the Qinghai-Tibet Plateau. Journal of Geophysical Research: Atmospheres, 125, e2020JD032588. https://doi.org/10.1029/2020JD032588

Lindstrom, G., Bishop, K., and Lofvenius, M. O. Soil frost and runoff at Svartberget, northern Sweden—measurements and model analysis. Hydrol. Process. 16, 3379–3392 (2002)

Liu, Y., Zhao, L., and Li, R. (2013). Simulation of the soil water-thermal features within the active layerin Tanggula region, Tibetan plateau, by using SHAW model. J. Glaciol. Geocryol. 35, 280–290.

Lyon, S. W., Destouni, G., Giesler, R., Humborg, C., Mörth, M., Seibert, J., Karlsson, J., and Troch, P. A.: Estimation of permafrost thawing rates in a sub-arctic catchment using recession flow analysis, Hydrol. Earth Syst. Sci., 13, 595–604, https://doi.org/10.5194/hess-13-595-2009, 2009.

Ma, R. Hydrological connectivity from glaciers to rivers in the Qinghai–Tibet Plateau: roles of suprapermafrost and subpermafrost groundwater. Hydrol. Earth Syst. Sci., 21, 4803–4823, 2017

McNamara, J.P.; Kane, D.L.; Hinzman, L.D. An analysis of streamflow hydrology in the Kuparuk River Basin, Arctic Alaska: A nested watershed approach. J. Hydrol. 1998, 206, 39–57.

Muster, S., Langer, M., Heim, B., Westermann, S., and Boike, J. (2012). Subpixel heterogeneity of ice-wedge polygonal tundra: a multi-scale analysis of land cover and evapotranspiration in the Lena River Delta, Siberia. Tellus B 64, 17301. doi:10.3402/tellusb.v64i0.17301

Nash, J. and Sutcliffe, J.V. (1970) River Flow Forecasting through Conceptual Models Part I—A Discussion of Principles. Journal of Hydrology, 10, 282-290. http://dx.doi.org/10.1016/0022-1694(70)90255-6

Nyberg, L. Soil frost effects on soil water and runoff dynamics along a boreal forest transect: 1. Field investigations. Hydrol. Process. 15, 909–926 (2001)

Niu, G.-Y. and Yang, Z.-L.: Effects of frozen soil on snowmelt runoff and soil water storage at a continental scale, J. Hydrometerol., 7, 937–952, 2006

Niu L, Ye B S, Li J, et al. Effect of permafrost degradation on hydrological processes in typical basins with various permafrost coverage in Western China. Sci China Earth Sci, 2010, doi: 10.1007/s11430-010-4073-1

Nitze, I., Grosse, G., Jones, B.M. et al. Remote sensing quantifies widespread abundance of permafrost region disturbances across the Arctic and Subarctic. Nat Commun 9, 5423 (2018). https://doi.org/10.1038/s41467-018-07663-3

Oleson, K., Lawrence, D., Bonan, G., Drewniak, B., Huang, M., Koven, C., Levis, S., Li, F., Riley, W., Subin, Z., Swenson, S., Thornton, P., Bozbiyik, A., Fisher, R., Heald, C., Kluzek, E., Lamarque, J.-F., Lawrence, P., Leung, L., Lipscomb, W., Muszala, S., Ricciuto, D., Sacks, W., Sun, Y., Tang, J., and Yang, Z.-L.: Technical description of version 4.5 of the Community Land Model (CLM), Boulder, Colorado, 2013.

Osuch, M. Diagnosis of the hydrology of a small Arctic permafrost catchment using HBV conceptual rainfall-runoff model. Hydrology Research, 2019

Pan, X. C., Yu, Q. H., You, Y. H., Chun, K. P., Shi, X. G., and Li, Y. P. (2017). Contribution of supra-permafrost discharge to thermokarst lake water balances on the northeastern Qinghai-Tibet Plateau. J. Hydrol. 555, 621–630. doi:10.1016/j.jhydrol.2017.10.046

Pianosi, F. and Wagener, T. Understanding the time-varying importance of different uncertainty sources in hydrological modelling using global sensitivity analysis. Hydrol. Process. 30, 3991–4003 (2016)

Ran Y, Li X, Cheng G, Nan Z, Che J, Sheng Y, Wu Q, Jin H, Luo D, Tang Z, Wu X. 2021. Mapping the permafrost stability on the Tibetan Plateau for 2005–2015. Science China Earth Sciences, 64(1): 62–79

Savenije, H.H.G., HESS Opinions: "The art of hydrology". Hydrol. Earth Syst. Sci., 13, 157–161, 2009

Savenije, H.H.G., 2010. HESS Opinions "Topography driven conceptual modelling (FLEXTopo)". Hydrol. Earth Syst. Sci. 14 (12), 2681–2692. https://doi.org/10.5194/hess-14-2681-2010.

Seibert, J., and J. J. McDonnell, On the dialog between experimentalist and modeler in catchment hydrology: Use of soft data for multicriteria model calibration, Water Resour. Res., 38(11), 1241, doi:10.1029/2001WR000978, 2002.

Shanley and Chalmers, A. The effect of frozen soil on snowmelt runoff at Sleepers River, Vermont. Hydrol. Process. 13, 1843±1857 (1999)

Sivapalan, M., Bloeschl, G., Zhang, L., and Vertessy, R. Downward approach to hydrological prediction. Hydrol. Process. 17, 2101–2111 (2003)

SjöBerg, Y. , Frampton, A. , & Lyon, S. W. . (2013). Using streamflow characteristics to explore permafrost thawing in northern swedish catchments. Hydrogeology Journal, 21(1), 121-131.

Sokolov, K.; Fedorova, L.; Fedorov, M. Prospecting and Evaluation of Underground Massive Ice by Ground-Penetrating Radar. Geosciences 2020, 10, 274.

https://doi.org/10.5194/hess-2021-264
Preprint. Discussion started: 25 May 2021

Streletskiy, D. "Permafrost hydrology in changing climatic conditions: seasonal variability of stable isotope composition in rivers in discontinuous permafrost." Environmental Research Letters 10.9(2015):095003.

Sun, A., Quantified hydrological responses to permafrost degradation in the headwaters of the Yellow River (HWYR) in High Asia. Science of the Total Environment 712 (2020) 135632 Permafrost Hydrology Research Domain: Process-Based Adjustment

Sun, Z., Zhao, L., Hu, G., Qiao, Y., Du, E., Zou, D., et al. (2019). Modeling permafrost changes on the Qinghai-Tibetan plateau from 1966 to 2100: a case study from two boreholes along the Qinghai-Tibet engineering corridor. Permafr. Periglac. Process. 31, 156–171. doi:10.1002/ppp.2022

Tananaev, N., Teisserenc, R., and Debolskiy, M. Permafrost Hydrology Research Domain: Process-Based Adjustment. Hydrology, 2020, 7, 6; doi:10.3390/hydrology7010006

Wagener, T. Towards reduced uncertainty in conceptual rainfall-runoff modelling: Dynamic identifiability analysis. Hydrol. Process. 17, 455–476 (2003)

Walvoord, M. A., and Kurylyk, B. L. (2016). Hydrologic impacts of thawing permafrost-A review. Vadose Zone J. 15. doi:10.2136/vzj2016.01.0010

Wang, G. X.,Mao, T. X., Chang, J., Song, C. L., and Huang, K. W. (2017). Processes of runoff generation operating during the spring and autumn seasons in a permafrost catchment on semi-arid plateaus. J. Hydrol. 550, 307–317. doi:10.1016/j.jhydrol.2017.05.020

Wang, L. Frozen soil parameterization in a distributed biosphere hydrological model. Hydrol. Earth Syst. Sci., 14, 557–571, 2010

Wang, P., Huang, Q., Pozdniakov, S.P., Liu, S., Ma, N., Wang, T., Zhang, Y., Yu, J., Xie, J., Fu, G. Potential role of permafrost thaw on increasing Siberian river discharge. Environmental Research Letters (2021) 16, 034046

Wang Q F, Jin H J, Zhang T J, et al. Active layer seasonal freeze-thaw processes and influencing factors in the alpine permafrost regions in the upper reaches of the Heihe River in Qilian Mountains (in Chinese). Chin Sci Bull, 2016, 61: 2742–2756, doi: 10.1360/N972015-01237

Wang, T., Dawen Yang, Yuting Yang, Shilong Piao, Xin Li, Bojie Fu, Guodong Chen, 2020. Permafrost thawing puts the frozen carbon at risk over the Tibetan Plateau. Science Advances, 6, eaaz3513.

Wang, Y. Frozen ground degradation may reduce future runoff in the headwaters of an inland river on the northeastern Tibetan Plateau. Journal of Hydrology 564 (2018) 1153–1164

Watson, V. , Kooi, H. , & Bense, V. . (2013). Potential controls on cold-season river flow behavior in subarctic river basins of siberia. Journal of Hydrology, 489, 214-226.

Woo, M-K. Permafrost Hydrology (2012), Springer, 5

https://doi.org/10.5194/hess-2021-264
Preprint. Discussion started: 25 May 2021

Hydrology and Earth System Sciences
Open Access
EGU
Discussions

Wu, T. H., Li, S. X., Cheng, G. D., and Nan, Z. T. (2005). Using ground-penetrating radar to detect permafrost degradation in the northern limit of permafrost on the Tibetan Plateau. Cold Reg. Sci. Technol. 41, 211–219. doi:10.1016/j.coldregions.2004.10.006

Xiao, Y. Representing permafrost properties in CoLM for the Qinghai–Xizang (Tibetan) Plateau. Cold Regions Science and Technology 87 (2013) 68–77

Yang, Y., Chen, R., Ye, B., Heat and water transfer processes on the typical underlying surfaces of frozen soil in cold regions (I): model comparison. Journal of Glaciology and Geocryology, 2013, 35(60): 1545-1554

Yang, Y. Z.,Wu, Q. B., Jin, H. J., Wang, Q. F., Huang, Y. D., Luo, D. L., et al. (2019). Delineating the hydrological processes and hydraulic connectivities under permafrost degradation on Northeastern Qinghai-Tibet Plateau, China. J. Hydrol. 569, 359–372. doi:10.1016/j.jhydrol.2018.11.068

Ye, B., D. Yang, Z. Zhang, and D. L. Kane (2009), Variation of hydrological regime with permafrost coverage over Lena Basin in Siberia, J. Geophys. Res., 114, D07102, doi:10.1029/2008JD010537.

Zhang, R. Can multi-objective calibration of streamflow guarantee better hydrological model accuracy? Journal of Hydroinformatics, 20.3, 2018

Zhang, T.; Frauenfeld, O.; Serreze, M.; Etringer, A. Spatial and temporal variability in active layer thickness over the Russian Arctic drainage basin. J. Geophys. Res. 2005, 110, D16101.

Zhang, X. High-resolution precipitation data derived from dynamical downscaling using the WRF model for the Heihe River Basin, northwest China. Theor Appl Climatol (2018) 131:1249–1259

Zhao, C., Yao, S., Li, Q. IOP Conf. Series: Earth and Environmental Science 428 (2020) 012063

Zhao L, Zou D, Hu G, et al. Changing climate and the permafrost environment on the Qinghai–Tibet (Xizang) plateau. Permafrost and Periglac Process. 2020;31: 396–405.

Zhou, J., Kinzelbach, W., Cheng, G., Zhang, W., He, X., and Ye, B. (2013). Monitoring and modeling the influence of snow pack and organic soil on a permafrost active layer, Qinghai-Tibetan Plateau of China. Cold Reg. Sci. Technol. 90-91, 38–52. doi:10.1016/j.coldregions.2013.03.003

Zou, D., Zhao, L., Wu, T., Wu, X., Pang, Q. and Wang, Z., 2014. Modeling ground surface temperature by means of remote sensing data in high-altitude areas: test in the central Tibetan Plateau with application of moderate-resolution imaging spectroradiometer Terra/Aqua land surface temperature and ground-based infrared radiometer. Journal of Applied Remote Sensing, 8.

Hydrology and Earth System Sciences
Open Access
Discussions

Figures

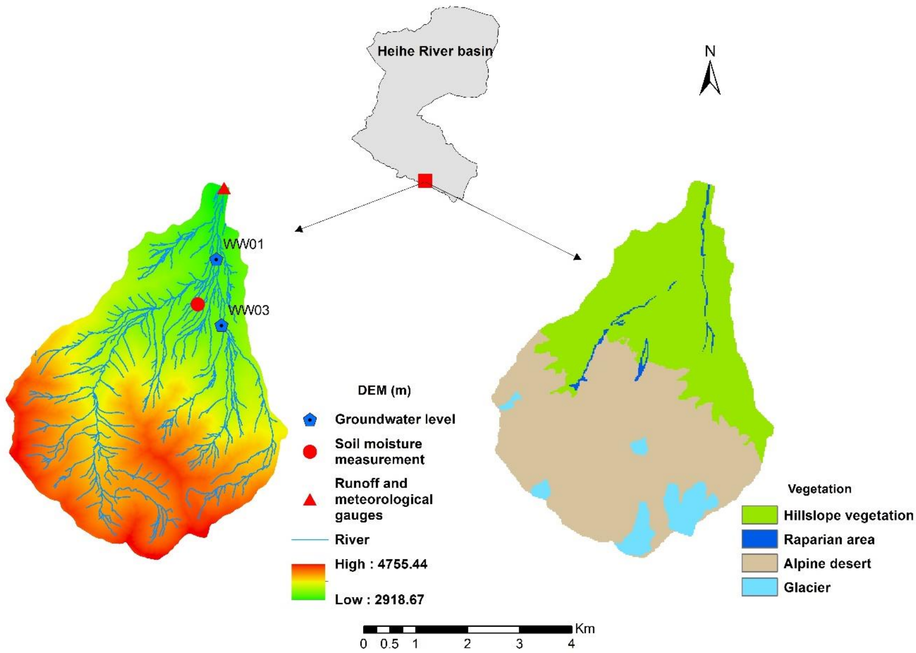

Figure 1. Sketch map of the Hulu catchment in the Heihe River basin, digital elevation model (DEM), river channel, groundwater level gauge station, soil moisture measurement site, runoff and meteorological gauge station, and land cover map.

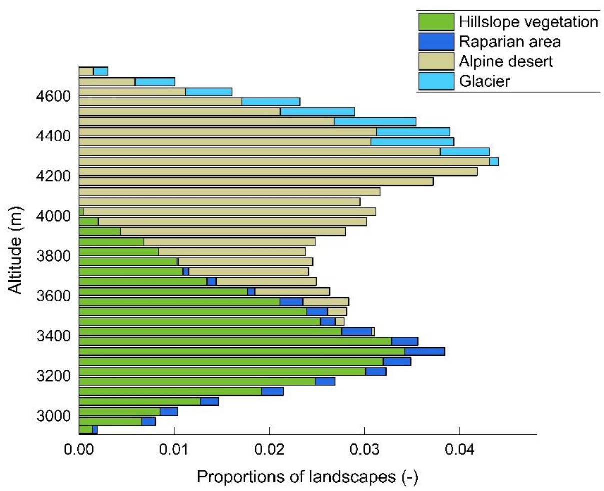

Figure 2. Landscape classification at different elevation bands (with 50m interval) of the Hulu catchment.

https://doi.org/10.5194/hess-2021-264
Preprint. Discussion started: 25 May 2021

Hydrology and Earth System Sciences
Discussions

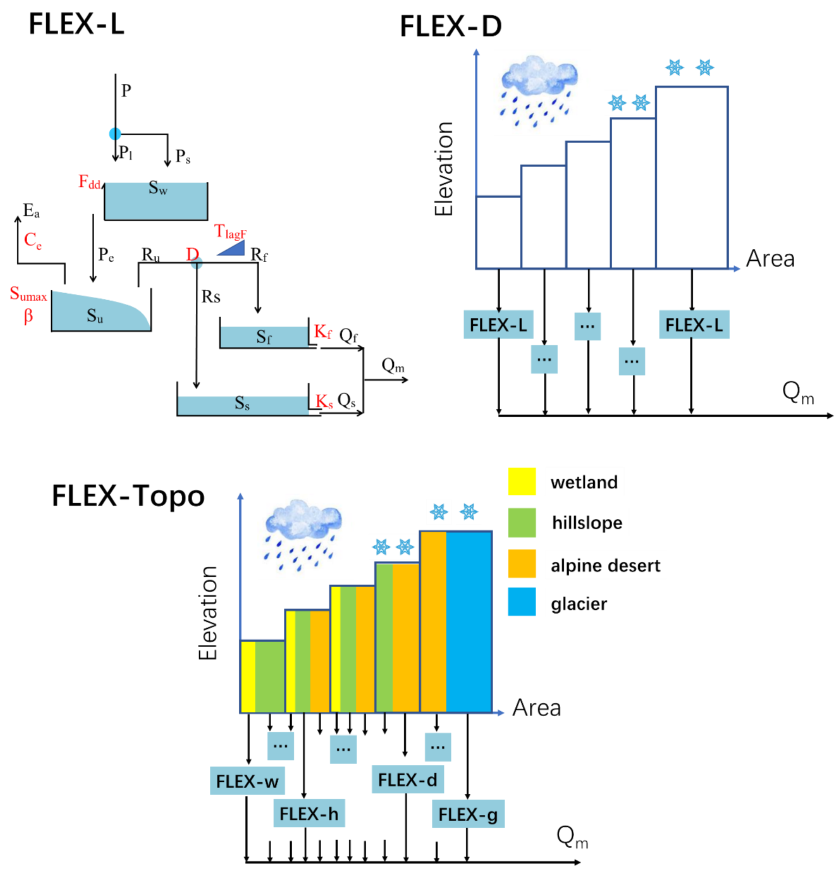

853

854 Fig 3. Model structures of FLEX-L, FLEX-D, and FLEX-Topo

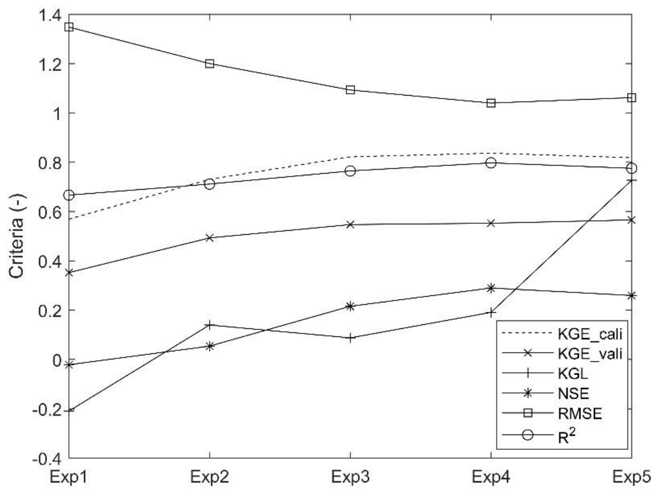

855

856 Figure 4. Stepwise modeling and their performance evaluated by different criteria in
857 calibration (KGE) and validation (KGE, KGL, NSE, RMSE, R^2).

https://doi.org/10.5194/hess-2021-264
Preprint. Discussion started: 25 May 2021

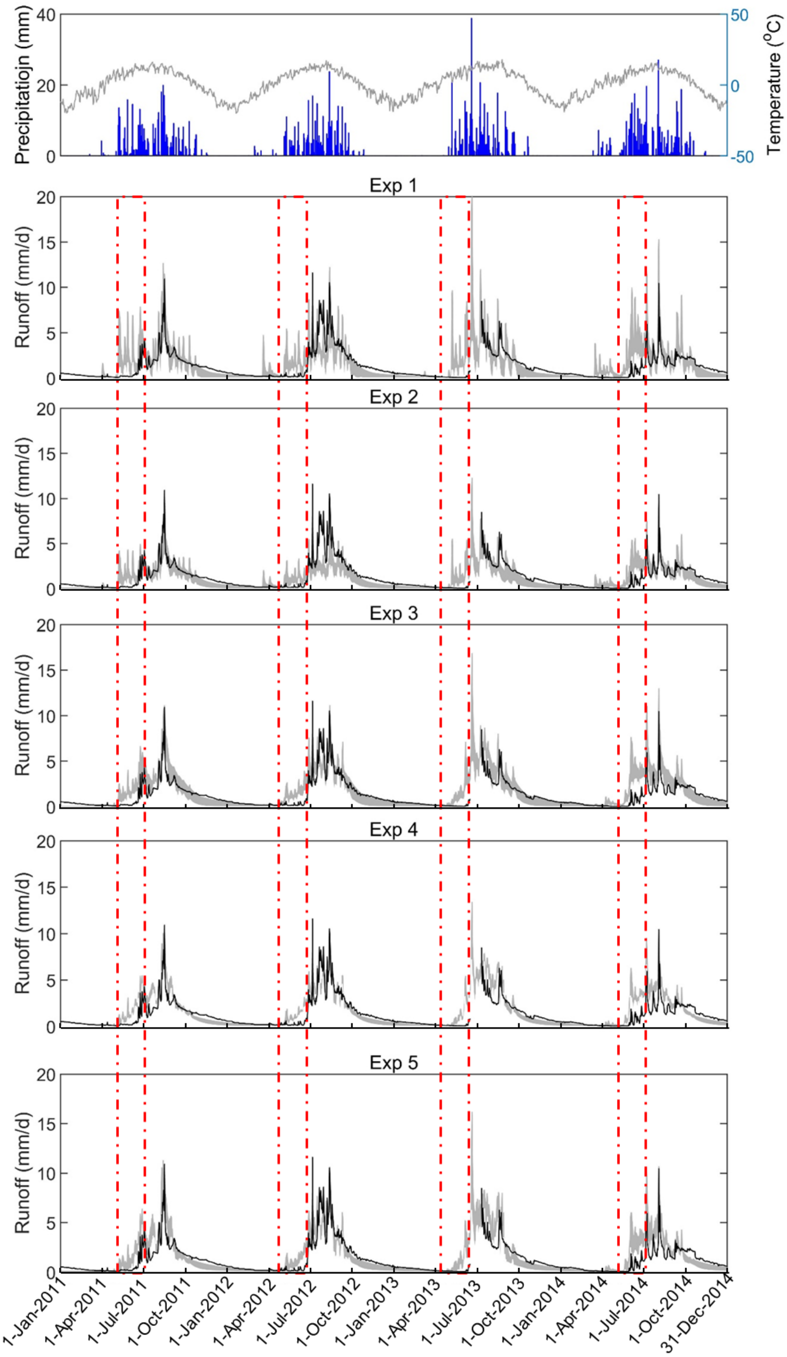

Figure 5. Modeling results of Exp1, Exp2, Exp3, and Exp4. Red dash boxes highlight the beginning of melt seasons when all models overestimated runoff.

https://doi.org/10.5194/hess-2021-264
Preprint. Discussion started: 25 May 2021

Hydrology and Earth System Sciences Discussions

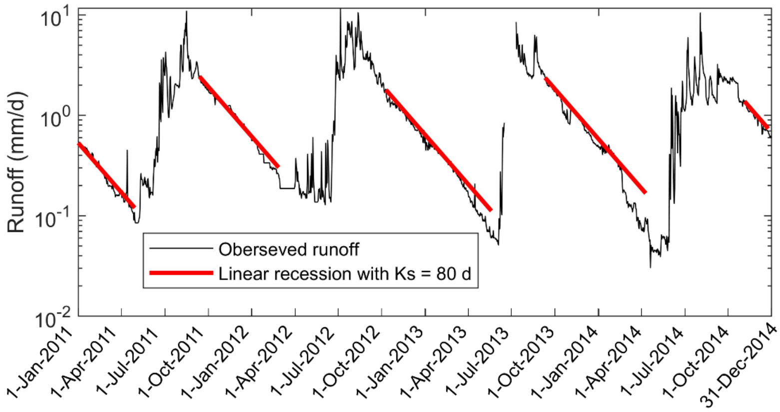

Figure 6. Groundwater recession in logmatic scale, with linear recession of Ks = 80 d.

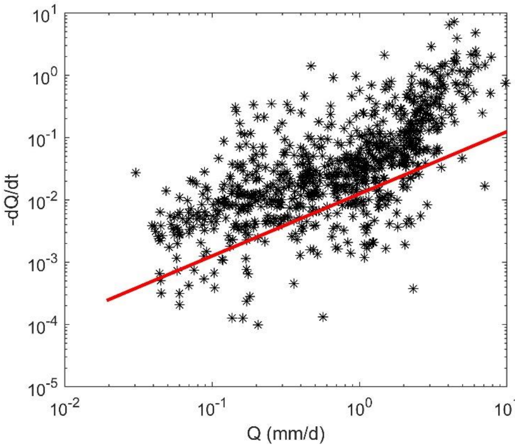

Figure 7. Data points observed Q plotted against $-dQ/dt$ of the Hulu catchment; the lower envelope line has a unit slope, in accordance with equation (5), and a value of the drainage time scale parameter Ks = 80 d. The upstream drainage area at this gauging station is 39 km^2.

https://doi.org/10.5194/hess-2021-264
Preprint. Discussion started: 25 May 2021

Hydrology and Earth System Sciences
Discussions

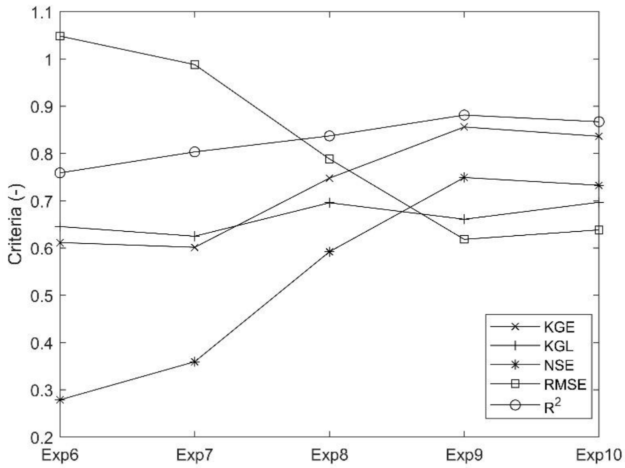

Figure 8. Model improvement in validation after allowing model parameter dynamics. Exp6 allows snow and glacier related parameters as temporal dynamic; Exp7 allows runoff generation related parameters as temporal dynamic; Exp8 allows runoff routine related parameters as temporal dynamic; Exp9 allows all parameters temporal dynamic; based on expert knowledge, Exp10 allows 4 parameters (D, S_{umax_V}, S_{umax_D}, F_{dd}) as temporal dynamic.

https://doi.org/10.5194/hess-2021-264
Preprint. Discussion started: 25 May 2021

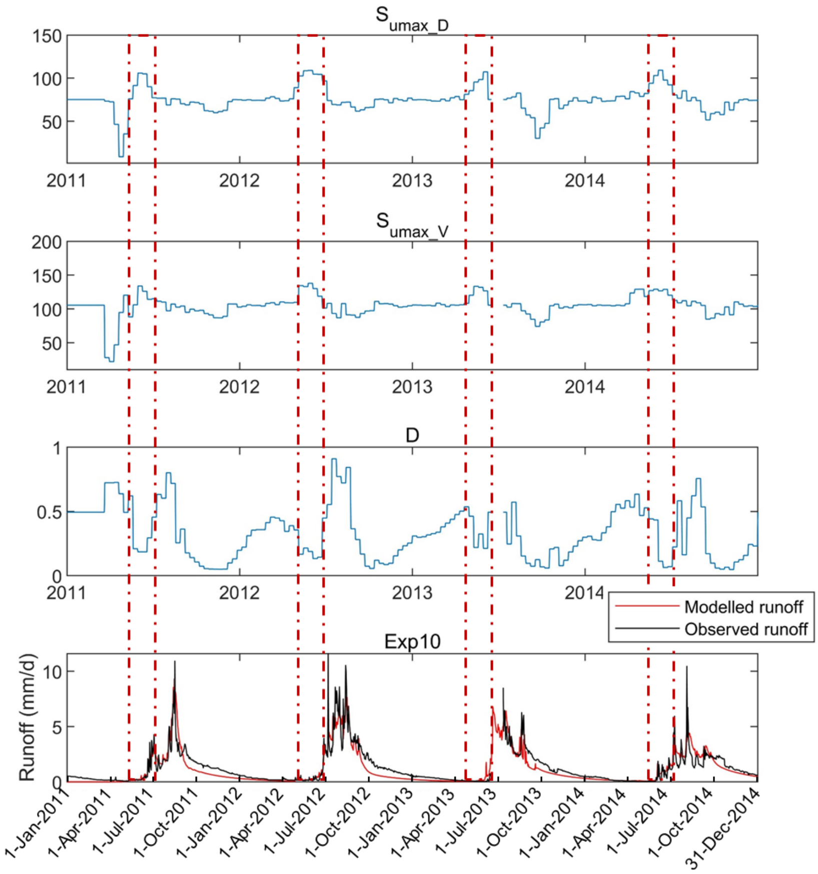

876

877 Figure 9. Temporal variation of three model parameters in Exp10, including S_{umax_D}, S_{umax_V}, D.
878 Runoff variation from 2011 to 2014.

879

https://doi.org/10.5194/hess-2021-264
Preprint. Discussion started: 25 May 2021

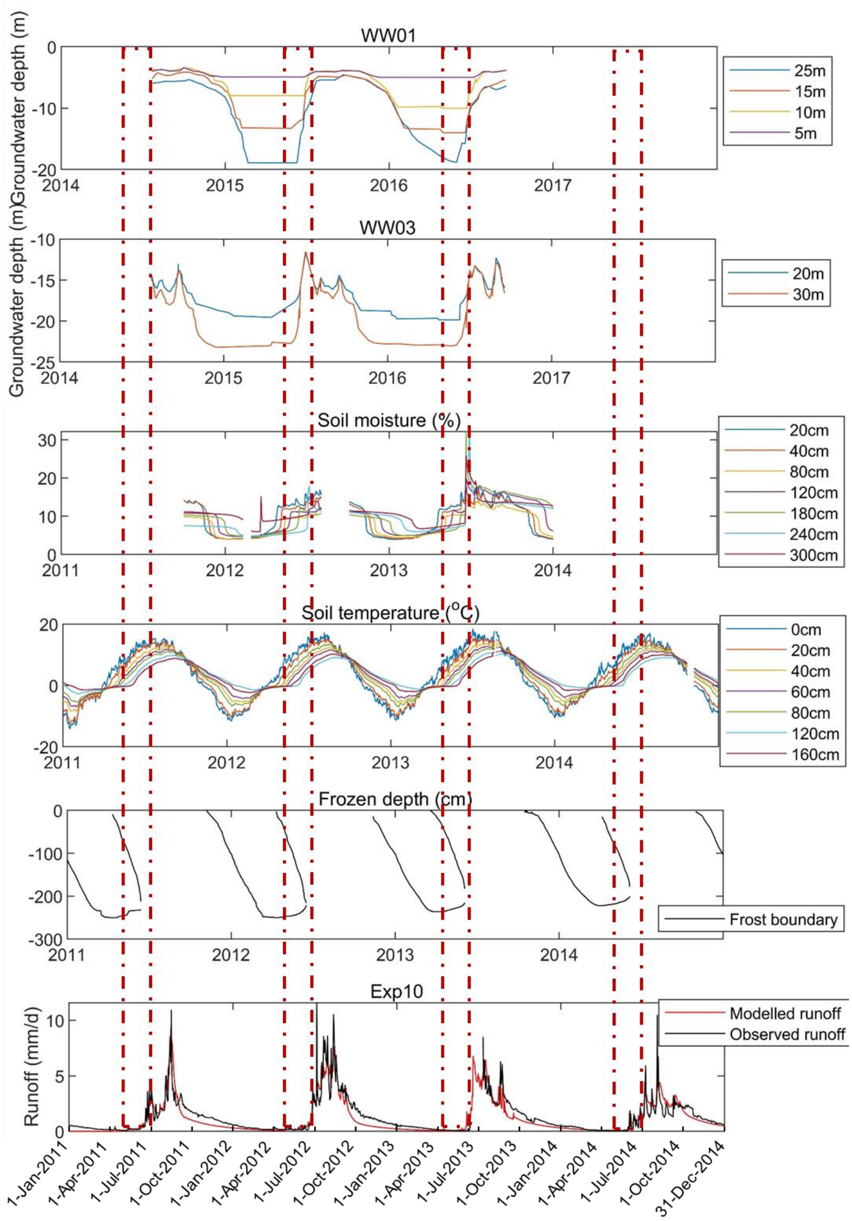

880

881 Figure 10. Observations of groundwater at WW01, with four wells of 5m, 10m, 15m and
882 25m depth; at WW03 with 2 wells of 20m and 30m depth. Groundwater observations were
883 conducted from 2014 to 2017. Temporal variation of soil moisture (20cm, 40cm, 80cm,
884 120cm, 180cm, 240cm, 300cm, during 2011-2014), soil temperature (0cm, 20cm, 40cm,
885 60cm, 80cm, 120cm, 160cm, during 2011-2014), frozen depth variation (during 2011-2014),
886 and modelled runoff in Exp10 (during 2011-2014).